Science Journal of Applied Mathematics and Statistics
2026; 14(1): 37-48
http://www.sciencepublishinggroup.com/j/sjams
doi: 10.11648/j.sjams.20261401.15

Multivariate Bayesian Spatio-Temporal Modeling of Malaria Incidence and Mortality in Kenya

Polycarp Okiagera Nyabuto[1, *], Anthony Wanjoya[1], Thomas Mageto[1], Anthony Ngunyi[2]

[1]Department of Statistics and Actuarial Science, Jomo Kenyatta University of Science and Technology, Nairobi, Kenya
[2]Department of Statistics and Actuarial Science, Dedan Kimathi University of Technology, Nyeri, Kenya

Email address:

polycarpn75@gmail.com (Polycarp Okiagera Nyabuto), awanjoya@gmail.com (Anthony Wanjoya), tttmageto@gmail.com (Thomas Mageto), anthonyngunyi@gmail.com (Anthony Ngunyi)
[*]Corresponding author

To cite this article:

Polycarp Okiagera Nyabuto, Anthony Wanjoya, Thomas Mageto, Anthony Ngunyi. (2026). Multivariate Bayesian Spatio-Temporal Modeling of Malaria Incidence and Mortality in Kenya. *Science Journal of Applied Mathematics and Statistics, 14*(1), 37-48.
https://doi.org/10.11648/j.sjams.20261401.15

Received: 7 December 2025; **Accepted:** 22 December 2025; **Published:** 20 January 2026

Abstract: In Kenya, malaria remains a major public health challenge, affecting a substantial proportion of the population and exhibiting pronounced spatial and temporal variability in transmission patterns. A comprehensive understanding of the spatial and temporal distribution of malaria incidence and mortality is therefore essential for the design and implementation of effective, targeted intervention strategies aimed at reducing disease burden and preventing malaria-related deaths. This study aimed to develop and apply a Multivariate Bayesian Spatio-Temporal modeling framework incorporating skew distributions to jointly analyze the spatio-temporal distribution of malaria incidence and mortality in Kenya. This proposed approach allowed for the explicit characterization of shared spatial structures and temporal trends, as well as the dependence between incidence and mortality across different counties and time periods. Parameter estimation was conducted using the Markov Chain Monte Carlo (MCMC) algorithm, which enabled sampling from the posterior distributions and facilitated robust statistical inference under uncertainty. The performance of the proposed model was assessed using established Bayesian model evaluation criteria which included the Widely Applicable Information Criterion (WAIC), the log pointwise predictive density (lppd), and the effective number of parameters (pWAIC). These metrics were used to evaluate model fit, predictive accuracy, and complexity, ensuring a balanced assessment of model performance. The results indicated that the multivariate Bayesian spatio-temporal model effectively captured the underlying spatial and temporal dependencies in malaria incidence and mortality across Kenya. The model successfully identified variations in risk across the Kenyan Counties and time periods, demonstrating its capacity to represent intricate malaria dynamics. Thus, this study findings highlight the utility of multivariate Bayesian spatio-temporal modeling as a powerful tool for understanding malaria transmission patterns and for informing evidence-based, spatially targeted malaria control and prevention strategies in Kenya.

Keywords: Bayesian, Multivariate, Spatial, Spatio-Temporal, Malaria Incidence, Malaria Mortality

1. Introduction

Malaria, a disease caused by *Plasmodium falciparum* and spread via bites from infected *Anopheles* mosquitoes, is a major global health threat that has devastating effects on human health particularly children under the age of five as well as pregnant women [1, 9]. In 2024, there were an estimated 263 million malaria cases globally and 597,000 deaths with the African continent bearing over 90% of both cases and fatalities [6]. In East Africa, and Kenya specifically, malaria is a top contributor to morbidity and mortality despite years of intervention with an incidence rate of 59 cases per 1,000 population [26] and a mortality rate of 0.21 deaths per 1,000 individuals [2]. The distribution of malaria is highly uneven throughout the country, particularly in the Western and Coastal Kenya Counties experiencing the heaviest

transmission burden.

Spatio-temporal models have become a vital approach in unraveling the intricate patterns of disease occurrence in epidemiology, as they allow for a simultaneous analysis of both spatial and temporal variability [4]. These models support the identification of high-risk areas, improve outbreak prediction, and facilitate the evaluation of intervention strategies over time and space [33]. In particular, Bayesian spatio-temporal models have been developed to help quantify spatial and spatio-temporal patterns of disease occurrence in epidemiology as with the case of conditional autoregressive (CAR) models [34].

Against this backdrop, this study applied the Multivariate Conditional Autoregressive modeling technique to develop a multivariate spatial-temporal skew model for analyzing spatial and spatio-temporal correlation of malaria incidence and mortality in Kenya thus offering deeper insights into the spatial and temporal distribution of malaria incidence and mortality in Kenya. This method enabled the detection of regions and time periods with elevated malaria risk, shedding light on the dynamic relationship between incidence and associated mortality.

2. Literature Review

This section explores key methodological approaches and advancements in spatial and spatio-temporal modeling, with a focus on malaria mapping. Studies such as Aheto *et al.* (2024) examined spatio-temporal patterns of malaria risk among children under five years of age in Ghana between 2016 and 2021 [3], employing Bayesian hierarchical models to account for spatial dependence and temporal trends. This approach complements the work of Apeagyei *et al.* (2024) [5], who investigated geographical inequalities in malaria outcomes and spending across 40 malaria-endemic countries from 2010 to 2020 using longitudinal secondary data and inequality metrics. While the latter provides important macro-level insights into disparities between burden and financing, its reliance on aggregated national data limits the ability to capture fine-scale spatial heterogeneity, which is addressed more explicitly in localized spatio-temporal studies.

Bationo *et al.* (2021) utilized remote-sensing-derived meteorological data to predict malaria cases in Burkina Faso [7], demonstrating the importance of climatic drivers in shaping malaria transmission. This aligns with Bisanzio *et al.* (2015) [8], who explored spatio-temporal heterogeneity in malaria risk using hospital surveillance data in coastal Kenya. However, while these studies integrate environmental covariates, they largely focus on predictive associations and do not explicitly model latent spatial processes, potentially underestimating unobserved heterogeneity.

Gopal *et al.* (2019) further expanded understanding of spatial factors influencing malaria occurrence and prevention measures in Kenya [10], while Gwitira *et al.* (2020) [11] applied spatial and spatio-temporal methods to malaria cases in Zimbabwe. Kamau *et al.* (2021) [13] and Kang *et al.* (2018) [14] investigated malaria trends in Kenya and Madagascar, respectively, using health facility data and national malaria indicator surveys. Although these data sources enhance temporal coverage and representativeness, many of these analyses treat spatial dependence implicitly or rely on exploratory spatial techniques rather than fully specified spatio-temporal models.

Katale and Gemechu (2023) [15] and Katile *et al.* (2022) [16] extended this line of inquiry by analyzing spatio-temporal variation in malaria incidence in Namibia and Mali, respectively. Similarly, Khagayi *et al.* (2017) [17] conducted Bayesian spatio-temporal modeling to link malaria incidence and mortality in Western Kenya, offering robust uncertainty quantification. Khan *et al.* (2023) [18], however, shifted focus toward the overlap of dengue, chikungunya, and malaria infections among children in Kenya, highlighting the growing relevance of co-endemic disease dynamics but with limited spatial modeling depth.

Further contributions by Kimuyu (2021) [19] and Kitawa *et al.* (2023) [20], who examined malaria vector invasion in Kenya and spatio-temporal variations in malaria risk in Ethiopia, respectively, underscore the importance of integrating entomological and spatial data. Liu *et al.* (2023) [21] provided a spatio-temporal assessment of malaria transmission intensity in Cambodia, while Maiti and Roy (2024) [22] and Mandal and Mondal (2024) [23] focused on co-occurring malaria species and the joint spatio-temporal dynamics of malaria and dengue in India. These studies demonstrate increasing methodological sophistication but remain largely context-specific, limiting cross-setting generalizability.

In Gabon, Mougeni *et al.* (2024) [24] applied Bayesian spatio-temporal models to analyze malaria prevalence among children, paralleling the work of Muzame *et al.* (2024) [25], who examined malaria prevalence in resource-limited settings in Kenya. While both studies provide valuable insights into childhood malaria risk, they primarily focus on prevalence outcomes without jointly modeling incidence or mortality.

The exploration of environmental drivers by Nyawanda *et al.* (2024) [26], who examined climatic and non-climatic factors affecting malaria mortality in Kenya, further enhances understanding of malaria distribution. Odhiambo *et al.* (2020) [27] reviewed spatial and spatio-temporal methods for malaria risk mapping, highlighting methodological gaps related to scale, uncertainty, and outcome integration. Ogunsakin *et al.* (2024) [28] utilized GIS techniques to investigate environmental inequalities in malaria prevalence in Nigeria, offering intuitive visualizations but limited inferential capacity.

Building on these spatial modeling efforts, Rotejanaprasert *et al.* (2023) [30] projected malaria elimination in Thailand, while Sangaré *et al.* (2022) [31] and Selemani *et al.* (2015) [32] analyzed spatial-temporal malaria patterns in Burkina Faso and Tanzania, respectively. Despite these advances, many existing studies either focus on single outcomes, rely on exploratory spatial methods, or do not fully integrate spatial and temporal dependencies within a unified modeling framework.

In this context, the present study contributes novel insights by applying an integrated spatial and spatio-temporal modeling approach that jointly captures fine-scale spatial heterogeneity and temporal dynamics by simultaneously examining malaria incidence and mortality within a single coherent framework.

3. Methodology

This study adopted a Multivariate Bayesian Spatio-Temporal modeling framework to develop a skew multivariate spatio-temporal model for analyzing malaria incidence and mortality in Kenya.

3.1. Skew Distributions in Spatial Modeling

Skew distributions in spatial modeling account for asymmetries in data that traditional symmetric models fail to capture[7]. This study incorporated skewness into spatial models to enhance the robustness of inference in the presence of spatial heterogeneity in the modeling of malaria incidence and mortality in Kenya[30].

3.1.1. Skew-Elliptical Distribution

A skew-elliptical distribution generalize traditional symmetric distributions by allowing for asymmetry, enabling more accurate modeling of real-world data that may be uneven or skewed while preserving the underlying dependence structure [24]. Hamedani *et al.* (2023) introduced a new right-skewed one-parameter distribution designed for actuarial risk analysis and other applications from the elliptically symmetric distributions [12]. Thus, following this formulation, a skew-elliptical distribution of a k-dimensional random vector Y is given as:

$$f(y|\mu,\Sigma,\Delta,g^k) = 2^k f(y|\mu,\Sigma+\Delta^2,g^k)P(V>0), \quad (1)$$

where μ is a vector of location parameters, Σ is a covariance matrix, Δ is a diagonal matrix of skewness parameters with elements $\Delta = (\delta_1,\delta_2,\ldots,\delta_k)^T$, and

$$\begin{aligned} V &\sim \text{El}\left(\Delta(\Sigma+\Delta^2)^{-1}(y-\mu), I_k - \Delta(\Sigma+\Delta^2)^{-1}\Delta; g^k_{q(y_*)}\right), \\ g^k_a(u) &= \frac{\Gamma(k/2)}{\pi^{k/2}} \frac{g(a+u,2k)}{\int_0^\infty r^{\frac{k}{2}-1} g(a+r,2k)\,dr}, \end{aligned} \quad (2)$$

where $a>0$ and $q(y_* = (y-\mu)^\top(\Sigma+\Delta^2)^{-1}(y-\mu)$. This distribution is symbolically denoted as: $Y \sim \text{SE}(\mu,\Sigma,\Delta,g^k)$. If $k=1$ then $\Sigma=\sigma^2$, $\Delta=\delta$ and the distribution reduces to a univariate distribution. Thus the density of Y is:

$$f(y|\mu,\sigma^2,\delta,g^1) = \frac{2}{\sqrt{\sigma^2+\delta^2}} g^{(1)} \frac{(y-\mu)^2}{\sigma^2+\delta^2} F\left(\frac{\delta}{\sigma}\frac{y-\mu}{\sqrt{\sigma^2+\delta^2}}\middle|0,1;g^{(1)}_a\right), \quad (3)$$

where $g^1(u)$ and $g^{(1)}_a(u)$ are as defined above, and $a = \frac{(y-\mu)^2}{\sigma^2+\delta^2}$. The marginal probability density function of a subsets of Y is determined as $Y_i|Z>0$, not $Y_i|Z_i$; the marginal probability density function of m_1 components of Y is given as:

$$f(y^{m_1}|\mu^{m_1},\Sigma_{11},\Delta_{11},g^{m_1}) = 2^{m_1} f(y^{m_1}|\mu^{m_1},\Sigma_{11}+\Delta_{11},g^{m_1})P(V>0). \quad (4)$$

3.1.2. Skewed-t Distribution for Random Effects

Following the Besag-York-Mollie (BYM) Conditional Autoregressive model [29], let Y_i denote the malaria incidence/mortality in county i ($i = 1,\ldots,47$) for which $Y_i \sim \text{Poisson}(\mu_i)$ and $\log(\mu_i) = \beta_0 + X_i\beta + u_i + v_i$. In this case, X_i are the county specific malaria incidence/mortality covariates, β_0 is the intercept, β is a vector of regression coefficients for covariates in X_i, u_i is the unstructured random effect presumed to be normally distributed, $u_i \sim N(0,\sigma_v^2)$ and v_i is the spatially structured random effect for county i. Using the Intrinsic Conditional Autoregressive Normal Prior (ICAR-Normal) [14], the spatially structured random effects are modeled in this study as;

$$u_i|u_{-i} \sim \text{ICAR}N(\mu_u,\sigma_u^2) = N\left(\frac{\sum_{j\sim i}\omega_j u_j}{m_i}, \frac{\sigma_u^2}{m_i}\right) \quad (5)$$

where m_i is the number of neighbors of county i, $u_i|u_{-i}$ is the conditional distribution of u_i given all the other structured spatial components and $j \sim i$ if county j is a neighbor to county i, ω_j is the spatial weight matrix whose value is one if county j is a neighbor to county i and zero otherwise, so it can be dropped out in the formula as the study is considering only neighboring counties; and this weighting approach is used throughout this study.

Suppose y follows a skew-t distribution with parameter k, the ICAR-skew-t model for the spatially structured spatial random effects u_i is given by

$$u_i \sim N\left(\frac{\sum_{j\sim i} s_j}{m_i} + \delta_u w_i, \frac{\sigma_s^2}{\eta \times m_i}\right), \quad (6)$$

where $w_i \sim N(0,1)$ with $I(w_i>0)$, and the conditional distribution of s_i given s_{-i} is $s_i \mid s_{-i} \sim N\left(\frac{\sum_{j\sim i} s_j}{m_i}, \frac{\sigma_s^2}{m_i}\right)$. In this formulation, σ_s^2 denotes the variance of s_i, and δ_u represents the skewness parameter associated with the spatial effect.

3.2. Bayesian Hierarchical Skew-t Modeling

Bayesian hierarchical skew-t models provide a flexible and robust approach for analyzing data characterized by asymmetry, heavy tails, and multilevel dependence, by explicitly allowing for skewness and extreme observations within a coherent probabilistic framework[12]. This modeling

strategy improves inferential reliability by accounting for latent heterogeneity and fully propagating uncertainty across hierarchical levels, making it particularly appropriate in epidemiological analyses[24].

3.2.1. Univariate Hierarchical Skew-t Modeling

Let Y_i be the malaria incidence/mortality in county i ($i = 1, \ldots, 47$) with a Poisson distribution. The hierarchical modeling framework for the ICAR-skew-t model is presented in this study as;

$$\begin{gathered} Y_i \sim \text{Poisson}(\boldsymbol{\mu_i} = E_i R_i) \\ R_i = \theta_i \times h_i; h_i = \exp(\beta_0 + u_i + v_i + g_{jk} + \psi_{s,t,k}) \\ \log(\mu_i) = \log(E_i) + \log(\theta_i) + \log(h_i) \\ v_i \sim N(0, \sigma_v^2); \psi_{s,t,k} \sim N(0, \sigma_\psi^2); \theta \sim \text{Gamma}(a, b) \\ g_{jk} \sim ICAR(\sigma_g^2); u_i | u_i, \sigma_u^2, \delta_u, \\ w_i \sim N\left(\frac{\sum\limits_{j\sim i} s_j}{m_i} + \delta_u w_i, \frac{\sigma_s^2}{\eta \times m_i}\right) \end{gathered} \tag{7}$$

For this model formulation, $\sigma_v^2 \sim \text{IG}(\Omega, v)$, $\delta_u \sim N(0, \Gamma)$, $\sigma_s^2 \sim \text{IG}(\Omega, u)$, and the parameter k is assigned an exponential prior as $\sim \text{Exp}(k_0)\, \mathbb{I}(k > 2)$. In this case, p_i represents the weighted prevalence associated with Y_i^* for $i = 1, 2, \ldots, 52$. The conditional distribution of s_i given s_{-i} is assumed to be normally distributed with mean $\frac{\sum\limits_{j\sim i} s_j}{m_i}$ and variance $\frac{\sigma_s^2}{m_i}$. The variable w_i is distributed as a truncated normal $N(0, I)$ restricted to positive values, and η follows a gamma distribution with both shape and rate parameters equal to $\frac{k}{2}$.

3.2.2. Multivariate Hierarchical Skew-t Modeling

Letting $Y_i = (Y_{i1}, Y_{i2}, \ldots, Y_{ik})$ to be a k-dimensional random variable with a Poisson distribution, the hierarchical representation of malaria incidence/mortality mapping models assuming the random components follow the above skew elliptical distribution is also obtained in this study as;

$$\begin{gathered} Y_i \sim \text{Poisson}(\boldsymbol{\mu_i} = E_i \times R_i) \\ R_i = \theta_i \times h_i; h_i = \exp(\beta_0 + u_i + v_i + g_{jk} + \psi_{s,t,k}) \\ \log(\mu_i) = \log(E_i) + \log(\theta_i) + \log(h_i) \\ v_i \sim \text{MVN}(0, \Sigma_v); \psi_i \sim \text{MVN}(0, \Sigma_\psi) \\ \theta \sim \text{Gamma}(a, b); g_{jk} \sim MCAR(1, \Sigma_g); \\ u_i | u_{-i}, \Sigma_u, \Delta_u, w_{iu} \sim \text{N}_k\left(\frac{\Sigma_{j\sim i} s_j}{mi} + \Delta_u w_{iu}, \frac{\Sigma_s}{mi}\right) \end{gathered} \tag{8}$$

where $w_{iu} \sim \text{N}_k(0, I_k)$, $I(w_{iu} > 0)$ if $u_i | u_{-i}$ has a skew-normal distribution, $s_{i|s_{-i}} \sim \text{N}_k\left(\frac{\Sigma_{j\sim i} s_j}{mi}, \frac{\Sigma_s}{mi}\right)$, $\beta_i \sim \text{N}(\beta_0, \Lambda)$, $\Sigma_v \sim \text{IW}(\Omega, h)$, $\Delta_u \sim \text{N}(0, \Gamma)$ and $\Sigma_u \sim \text{IW}(D, h)$ where $i = 1, 2, \ldots, n$, Σ_g, Σ_ψ, Σ_u and Σ_v are covariances of the spatialy structured and the unstructured random effects, and $I(w_{iu} > 0)$ is a a characteristic function, IW is the Inverse Wishart Distribution.

3.3. Posterior Distribution

Posterior distribution in this study served as the foundation for making inferences and drawing conclusions about the spatial and temporal variation of malaria incidence and mortality in Kenya.

3.3.1. Bayesian Hierarchical Skew-t Model

Given the likelihood function and the specified prior distributions, [34] obtained the posterior distribution of the parameters, assuming conditional independence between the response variable and the hyper-parameters, as

$$\begin{aligned} p\big(\mu, \beta, u, v, \sigma_u^2, \sigma_v^2, \delta_u, w, k, \eta, s \mid y^*\big) &\propto L\big(y \mid \beta, u, v, \sigma_s^2, \sigma_v^2, \delta_u, w, s\big) \times P\big(\beta, u, v, \sigma_s^2, \sigma_v^2, \delta_u, w, k, \eta\big) \\ &= \prod_i p(y_i^* \mid \mu_i) \times p(w) p(\delta_u) \times p(k) p(\eta) \\ &\quad \times \prod_j p(\beta_j \mid \Lambda) p(\Lambda) \times p(s \mid \sigma_s^2) p(u \mid \sigma_s^2) p(\sigma_s^2) \\ &\quad \times p(v \mid \sigma_v^2) p(\sigma_v^2). \end{aligned} \tag{9}$$

3.3.2. Multivariate Hierarchical Skew-t Model

Under the assumption that the response variable is conditionally independent of the hyper-parameters, the joint posterior distribution for the multivariate hierarchical skew-t model is expressed as:

$$\begin{aligned} p(\mu_i, \beta_i, u_i, v_i, \Sigma_g, \Sigma_\psi, \Sigma_u, \Sigma_v, \delta_u, w_{iu} | y_i) &\propto L(y_i | \mu_i, \beta_i, u_i, v_i, \Sigma_g, \Sigma_\psi, \Sigma_u, \Sigma_v, \Delta_u, w_{iu}) \times \\ &\quad P(\beta_i, u_i, v_i, \Sigma_g, \Sigma_\psi, \Sigma_u, \Sigma_v, \Delta_u, w_{iu}) \\ &= \prod_i p(y_i | \mu_i) \prod_j (p(\beta_j | \Lambda) p(\Lambda)) \Theta. \end{aligned} \tag{10}$$

where $\Theta = p(u_i|\Sigma_u)p(\Sigma_u)p(v_i|\Sigma_v)p(\Sigma_v)\ p(g_i|\Sigma_g)p(\Sigma_g)p(\psi_i|\Sigma_\psi)p(\Sigma_\psi)\ p(w_{iu})p(\Delta_u)$.

Parameter estimation was carried out via the MCMC method, which necessitates deriving the full conditional distributions. Accordingly,the conditional distributions of the parameters are as;

$$\beta_i|\mu_i, \Sigma_u, \Sigma_v, y_i \sim N(A_\beta^{-1}a_\beta, A_\beta^{-1}) \tag{11}$$

where $A_\beta^{-1} = \Lambda^{-1} + \Sigma_v X^T X$ and $a_\beta = \Lambda^{-1}\beta_0 + X^T(\mu - \mu_i)/\Sigma_v$

$$u_i|u_{-i}, \Sigma_u, \Delta_u, w_{iu}, \Sigma_v, \mu_i, \beta_i \sim N\left(\frac{\gamma_v(\mu_i - X\beta_i) + \gamma_u(\sum_{j\sim i}\omega_{ij}(s_j + \Delta_u w_{iu}))}{\Sigma_v^{-1} + \gamma_u m_i}, \frac{1}{\Sigma_v^{-1} + \gamma_u m_i}\right) \tag{12}$$

where $\gamma_u = \Sigma_u^{-1}$,

$$\begin{gathered} v_i|\Sigma_u, \Sigma_v, \mu_i, \beta_i \sim N\left(\frac{\gamma_u(\mu_i - X\beta_i)}{\Sigma_v^{-1} + \gamma_u m_i}, \frac{1}{\Sigma_v^{-1} + \gamma_u m_i}\right), \\ w_{iu}|u_i, \Sigma_u, \Delta_u = N(A_w^{-1}a_w, A_w^{-1})I(w_i > 0) \end{gathered} \tag{13}$$

where $A_w = \Sigma_u\gamma_u m_i + 1$ and $a_w = \Delta_u\gamma_u u_i$.

Also,

$$\Delta_u|u_i, \Sigma_u, w_{iu} \sim N(A_{\Delta u}^{-1}a_{\Delta_u}, A_{\Delta_u}^{-1})$$

where

$$A_{\Delta_u} = \Gamma^{-1} + \sum_{i=1}^{n}\frac{w_{iu}^2}{\Sigma_u}$$

and

$$a_{\delta_u} = \sum_{i=1}^{n}\frac{w_{iu}\mu_i}{\Sigma_u}$$

for which

$$\begin{gathered} \Sigma_v|\mu_i, \beta_i, u_i, \mu_i = IW\left(\Omega + \sum_{i=1}^{n}(\mu_i - u_i - X\beta_i)(\mu_i - u_i - X\beta_i)^T, h + n\right) \\ \Sigma_u|\mu_i, \beta_i, u_i, \mu_i = IW(D + u'(D_w - W)u, k + n) \end{gathered} \tag{14}$$

where, D_w denoted a diagonal matrix with entries representing the number of neighboring regions for each county, while W corresponds to the spatial adjacency matrix.

4. Results and Discussion

This section presents the results of the proposed modeling framework, highlighting its performance in both univariate and multivariate settings. For the univariate case, the model captured the spatio-temporal dynamics of malaria incidence and mortality effectively accounting for local variability and temporal trends. In the multivariate case, the framework extended to jointly modeling malaria incidence and mortality thus allowing for the characterization of shared spatial and temporal structures and the interactions between malaria incidence and mortality.

4.1. Exploratory Spatial Data Analysis

In order to aid exploratory data analysis, the study used spatial descriptive statistics as presented in Table 1. The minimum malaria incidence and mortality were 0.00, indicating regions with either effective control measures or naturally low transmission. The mean malaria cases showed a minimum of 5, suggesting some cases even in less affected areas.

Table 1. *Descriptive Statistics of the Study Data.*

Variable	Min.	1st Qu.	Median	Mean	3rd Qu.	Max.
Malaria Incidence Rate	0.00	23.00	40.00	64.57	72.00	367.00
Malaria Mortality Rate	0.000	3.000	6.000	9.678	12.000	76.000

The quartile distribution highlights the variation across regions: for incidence, the first quartile is 23, the median 40, and the third quartile 72; for mortality, these values are 3, 6, and 12, respectively. This shows most regions have relatively low rates, though some experience higher burdens. Median values (40 for incidence and 6 for mortality) confirm malaria as a concern, though extreme cases are less frequent. Outliers are notable, with a maximum incidence rate of 367, mortality rate of 76 reflecting disproportionate impacts in certain regions. Figure 1 provides histograms and spatial map of malaria incidence and mortality rates in Kenya.

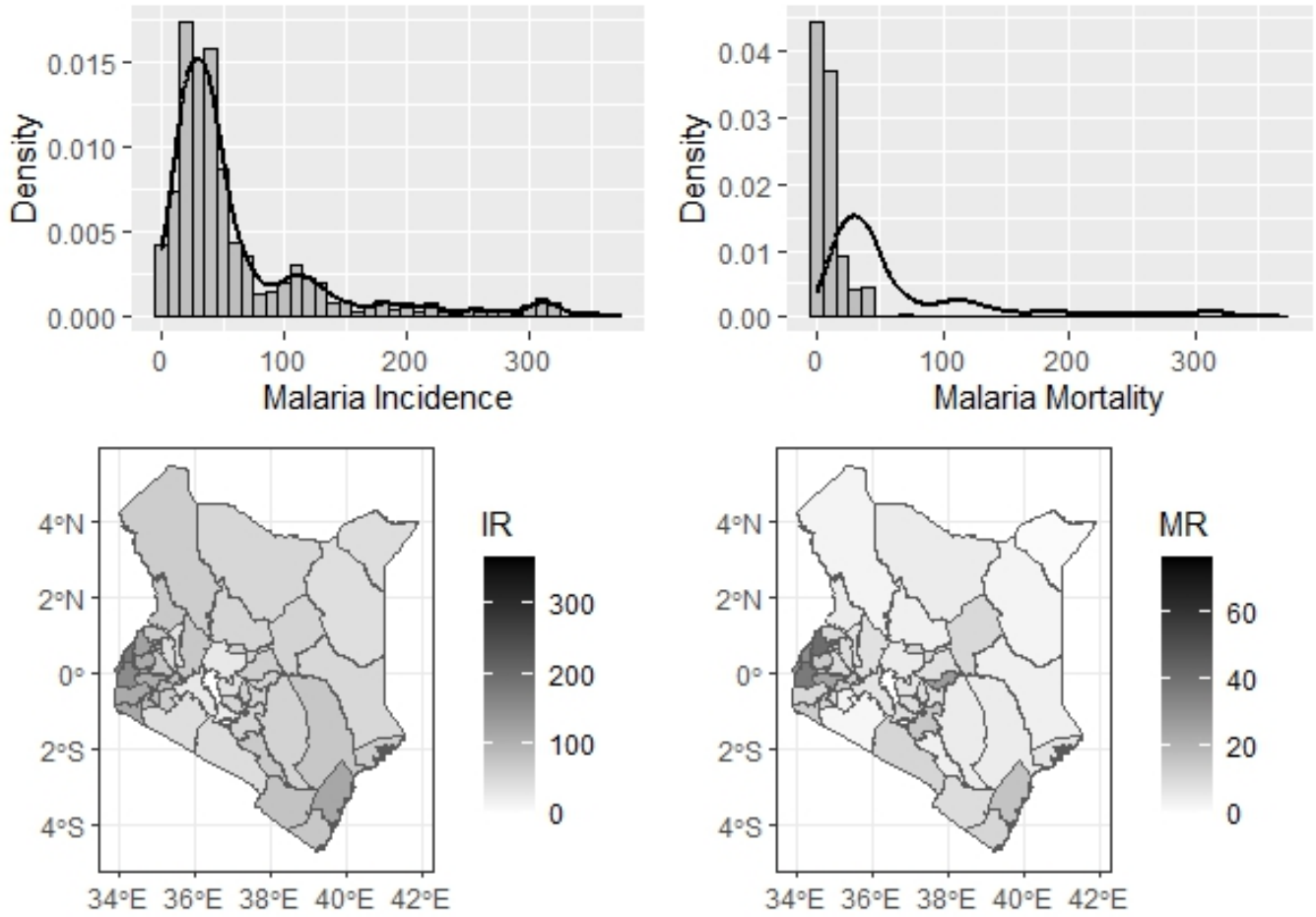

Figure 1. *Histogram of Malaria Incidence and Mortality Rates.*

The spatial distributions and density plots in Figure 1 indicate strong right-skewness in both malaria incidence and mortality, with most counties experiencing relatively low rates while a small number sustain disproportionately high burdens. The maps show these elevated incidence and mortality rates concentrated primarily in the western lake-endemic counties, including Siaya, Homa Bay, Kisumu, Migori, and Busia, and extending into parts of the coastal belt, while the central highlands and eastern interior counties remain consistently low. Mortality appeared more spatially localized than incidence, suggesting that although transmission is widespread within endemic zones, fatal outcomes may be driven by heterogeneities in healthcare access, prompt treatment, or population vulnerability.

4.2. Bayesian Skew-t Hierarchical Modeling

In the hierarchical spatial temporal modeling of malaria incidence and mortality rates in Kenya, this study first considered the univariate modeling and then the multivariate modeling.

4.2.1. Univariate Modeling of Malaria Incidence and Mortality Rates

The results from the univariate modeling of malaria incidence rates, as presented in Table 2, reveal insightful parameter estimates regarding the spatial-temporal dynamics of the disease. The intercept parameter a_0 had a mean of -1.9295, indicating a low baseline incidence rate with a narrow uncertainty range (-2.000 to -1.7719), reflecting stable baseline predictions. Temporal variability (dtg) had a mean of 0.3184, suggesting moderate fluctuations over time, with a credible range of 0.2169 to 0.5135.

Table 2. *Univariate Modeling of Malaria Incidence Rates Parameter Estimates.*

Parameter	Mean	SD	2.5% Percentile	97.5% Percentile
a_0	-1.9295	0.0925	-2.000	-1.7719
dtg	0.3184	0.1050	0.2169	0.5135
dtv	0.7373	0.2352	0.4950	1.1055
dtu	1.6361	0.3009	1.1611	2.2229
dtpsi	0.4708	0.0671	0.4016	0.7166
mspe	145.1742	35.3272	115.3825	263.5396

Spatial components are divided into correlated (dtu) and uncorrelated (dtv) factors. The correlated component (dtu) had a mean of 1.6361, indicating strong spatial correlation and a wider uncertainty range (1.1611 to 2.2229). In contrast, the uncorrelated component (dtv) had a lower mean of 0.7373 and a narrower range (0.4950 to 1.1055), reflecting less variability in areas without spatial correlation. The space-time interaction term (dtpsi) shows moderate interaction with a mean of 0.4708 and a credible range of 0.4016 to 0.7166, indicating spatial dependence in temporal changes. The mean squared predictive error (MSPE) of 145.1742, with a broad uncertainty range (115.3825 to 263.5396), highlights variability in predictive accuracy, emphasizing the model's challenges in generalization.

The univariate modeling results of malaria mortality rates, as displayed in Table 3, provide important insights into the spatial-temporal characteristics of the data. The intercept parameter (a_0) had a mean of -3.1541, indicating a low baseline for malaria mortality rates with a narrow uncertainty range (-3.5341 to -2.6492). Temporal variability (dtg) is modest, with a mean of 0.2966 and a credible interval of 0.1973 to 0.4312, reflecting consistent temporal patterns.

Table 3. *Univariate Modeling of Malaria Mortality Rates Parameter Estimates.*

Parameter	Mean	SD	2.5% Percentile	97.5% Percentile
a_0	-3.1541	0.3170	-3.5341	-2.6492
dtg	0.2966	0.0705	0.1973	0.4312
dtv	0.8778	0.1721	0.6285	1.2932
dtu	1.2733	0.5698	0.4647	2.3340
$dt\psi$	0.1296	0.0488	0.1000	0.2146
$mspe$	20.3556	2.3698	15.8252	25.5049

Spatially, uncorrelated variability (dtv) had a mean of 0.8778 and a moderate range (0.6285 to 1.2932). Correlated spatial variability (dtu) is stronger, with a mean of 1.2733, but a wider credible interval (0.4647 to 2.3340), indicating significant uncertainty. The space-time interaction term (dtpsi) is weak, with a mean of 0.1296 and a narrow range (0.1000 to 0.2146), showing limited interaction between spatial and temporal effects. The model's predictive accuracy is reasonable, with a mean squared predictive error (MSPE) of 20.3556 and a credible interval of 15.8252 to 25.5049.

Figure 2 presents the univariate temporal trends for malaria incidence and mortality rates from 2010 to 2022, ranging between 0.75 and 1.50.

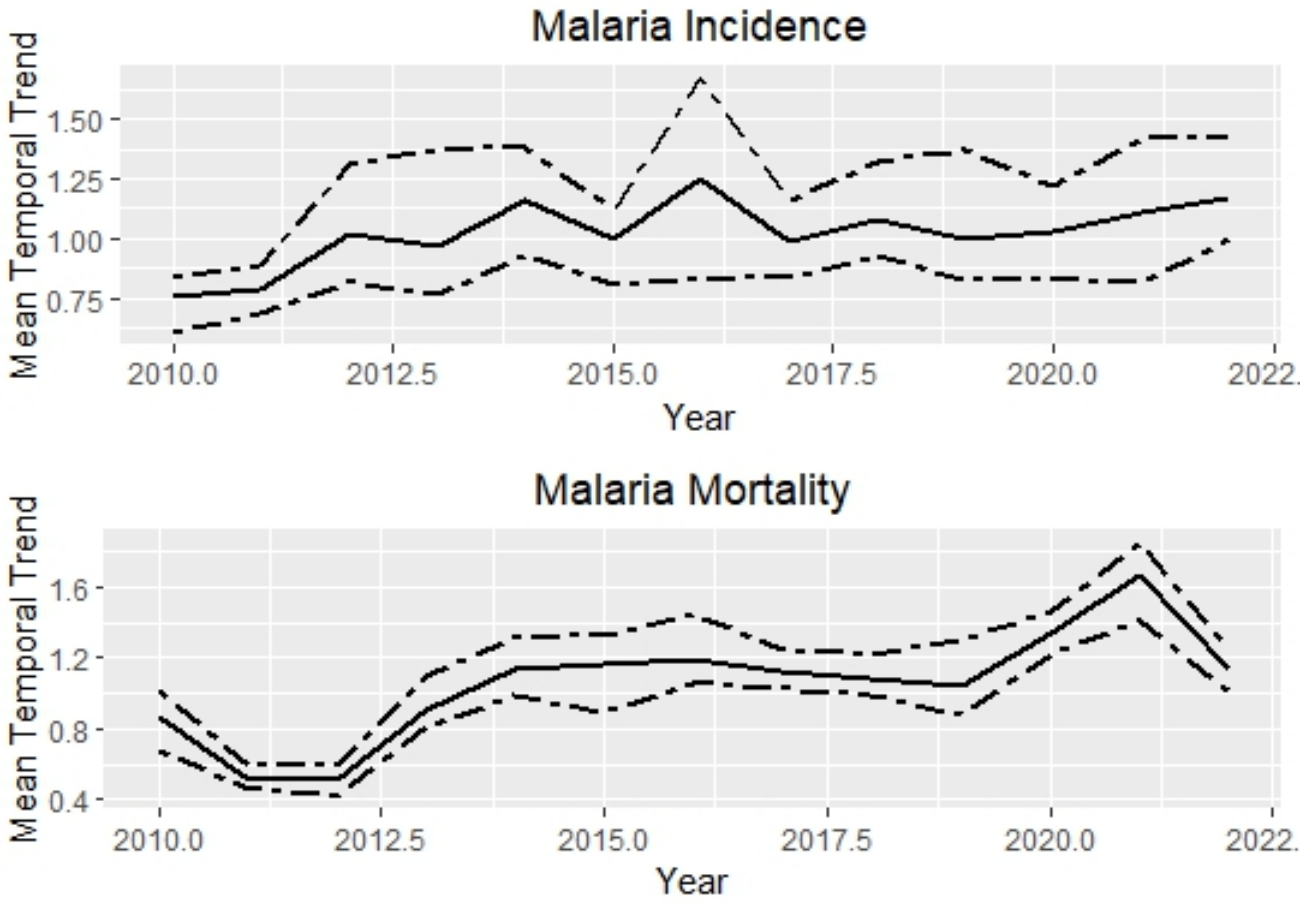

Figure 2. *Univariate Temporal trend for Malaria Incidence and Morality Rates.*

The solid line represents the mean trend, while dashed lines show the 95% confidence intervals (CI), indicating the likely range of true rates. From 2010 to 2012, incidence rates increase, peaking in 2012, followed by a decline through 2015, likely reflecting successful interventions or environmental changes. Between 2015 and 2018, the trend stabilizes with minor fluctuations. After 2018, rates rise again, peaking around 2020.

Figure 3 gives the Spatial trend and Exceedance Probabilities for Malaria Incidence and Mortality across Kenyan counties. It demonstrates marked spatial heterogeneity in malaria burden across Kenya, with high incidence, mortality, and exceedance probabilities concentrated in western lake-endemic counties (Siaya, Homa Bay, Kisumu, Migori, and Busia) and parts of the coastal and northeastern regions, while central highland counties (Nyeri, Kirinyaga, Murang'a, Kiambu, and Nyandarua) exhibit consistently low levels. Mortality generally mirrored incidence but showed localized hotspots in the northeast counties of Garissa and Mandera, suggesting differential vulnerability. The exceedance probability (Pr>1) reinforced these patterns, showing a high likelihood of above-average incidence and mortality in western Kenya and selected coastal/northeastern counties, contrasted with probabilities near zero across most highland and eastern interior counties, indicating sustained low transmission risk.

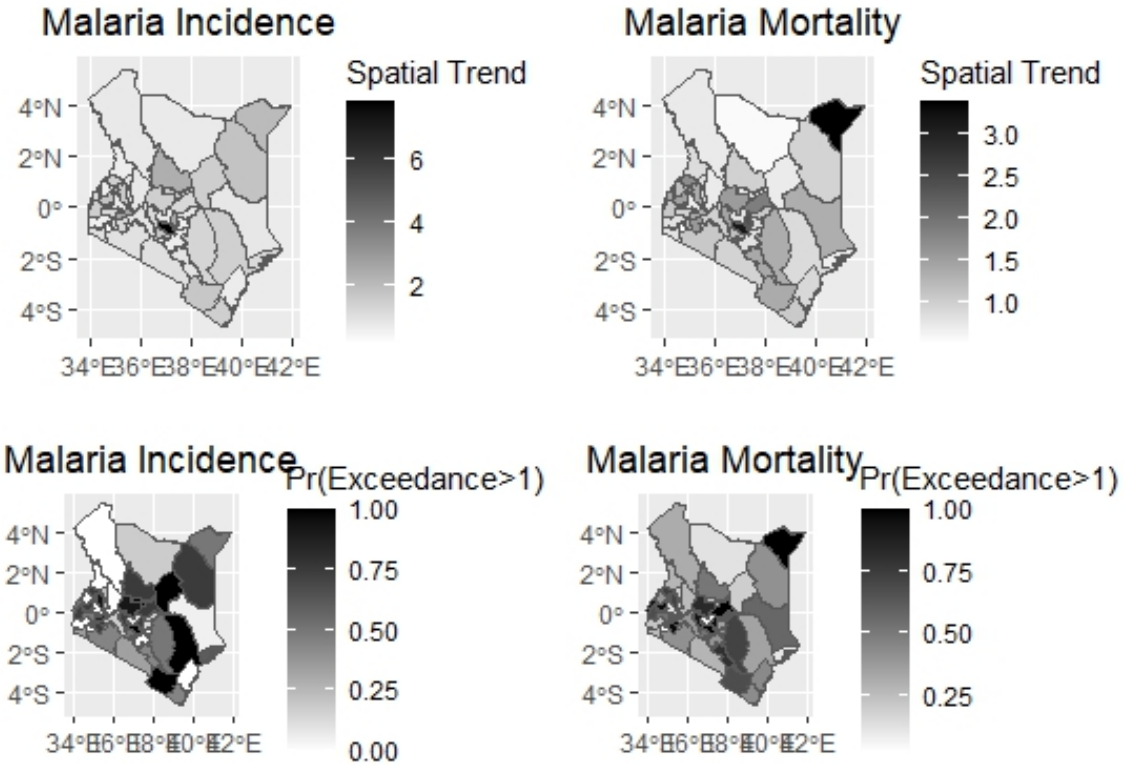

Figure 3. *Spatial trend and Exceedance Probabilities for Malaria Incidence and Mortality*

4.2.2. Multivariate Modeling of Malaria Incidence and Mortality Rates

The multivariate modeling results presented in Table 4 provide a comprehensive view of the spatial-temporal dynamics of malaria incidence and mortality. The baseline parameter for malaria mortality (a_{0m}) had a mean of -2.7293, reflecting low mortality rates, with a narrow credible interval (-3.1980 to -2.2141) indicating high precision. In contrast, the baseline for incidence (a_{0i}) is much lower, with a mean of -5.3243 and a wider interval (-6.6467 to -4.1798), suggesting greater variability but generally lower incidence rates.

Table 4. *Multivariate Modeling Parameter Estimates.*

Parameter	Mean	SD	2.5% Percentile	97.5% Percentile
a_{0m}	-2.7293	0.3377	-3.1980	-2.2141
dtu_m	1.1039	0.3871	0.4483	1.6658
dtv_m	1.2111	0.3304	0.7623	1.9130
$dtpsi_m$	0.1128	0.0222	0.1000	0.1512
dtg_m	1.1944	1.1455	0.2345	4.1802
a_{0i}	-5.3243	1.0264	-6.6467	-4.1798
dtv_i	2.6119	0.9276	1.4024	4.4747
$dtpsi_i$	1.8260	0.2875	1.5011	2.4359
dtu_i	2.8045	0.7291	1.5710	4.2374
dtg_i	2.6723	2.0249	0.5487	6.3579
$mspe_m$	20.7127	2.5375	16.8509	26.7017
$mspe_i$	220.6606	276.3378	116.2084	999.2930

Spatial components reveal distinct patterns. For mortality, the correlated component (dtu_m) had a mean of 1.1039, and the uncorrelated component (dtv_m) had a slightly higher mean of 1.2111, indicating moderate spatial variability. Incidence shows stronger spatial correlation, with dtu_i at 2.8045 and dtv_i at 2.6119, reflecting substantial spatial variation. Space-time interaction differs significantly. Mortality's interaction ($dtpsi_m$) is weak, with a mean of 0.1128, indicating minimal spatial-temporal dependence. Conversely, incidence's interaction ($dtpsi_i$) is much stronger, with a mean of 1.8260, highlighting pronounced space-time dynamics. Temporal components also vary. Mortality's temporal variation (dtg_m) had a mean of 1.1944, indicating moderate fluctuations, while incidence's (dtg_i) is higher at 2.6723, suggesting greater temporal variability. Predictive accuracy contrasts sharply. The mean squared predictive error (MSPE) for mortality ($mspe_m$) is low at 20.7127, indicating high accuracy. For incidence, however, $mspe_i$ is significantly higher at 220.6606, with considerable variability and uncertainty.

Figure 4 illustrates the multivariate temporal trend for malaria mortality and incidence rates from 2010 to 2022. From 2010 to 2015, malaria mortality rates increased, peaking in 2015, followed by a decline until 2017, likely due to improved health-care and control measures. Between 2017 and 2020, rates stabilized with minor fluctuations. Post-2020, mortality rates rose again, peaking around 2021, possibly due to changes in transmission dynamics, climate, health-care access, or socio-economic factors.

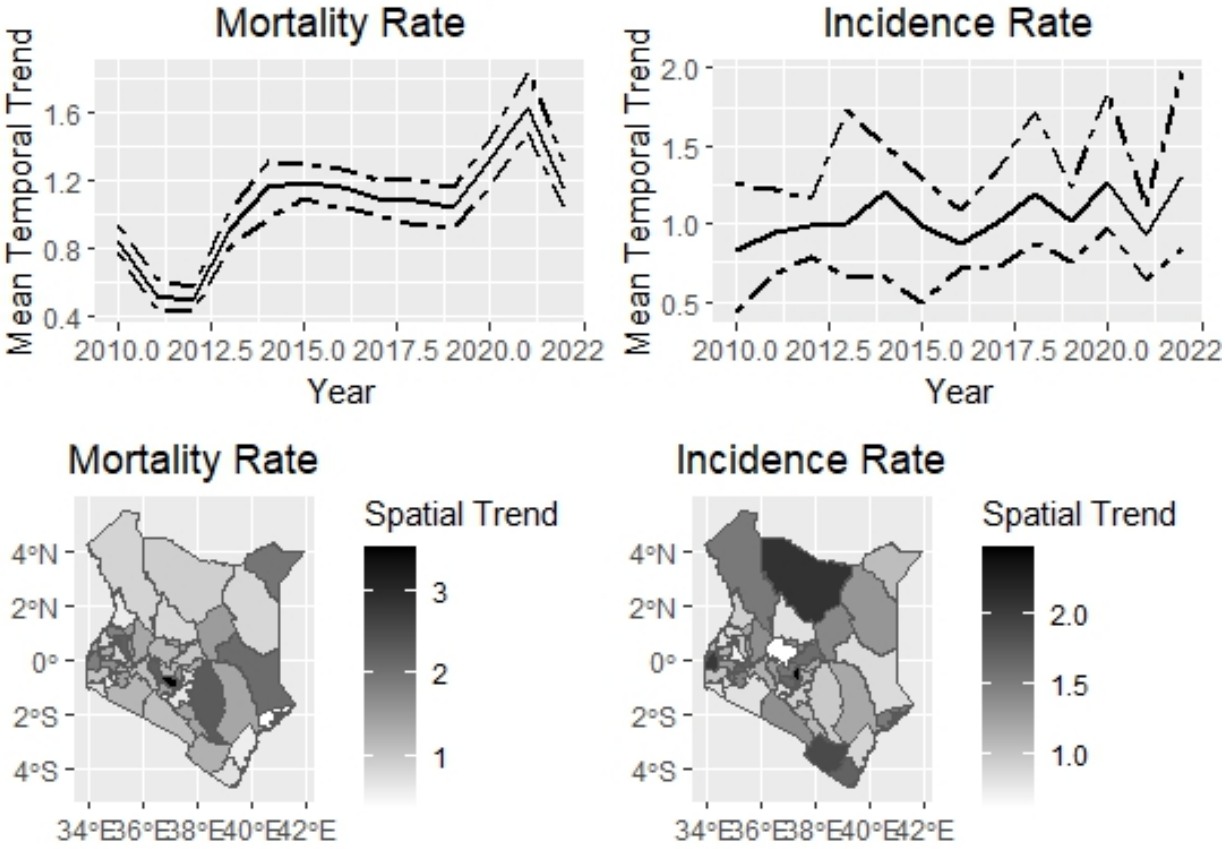

Figure 4. *Multivariate Temporal and Spatial trend for Malaria Mortality and Incidence.*

The spatial trend maps in Figure 4 for the Multivariate Spatio-Temporal Model reveal pronounced geographic structuring of both malaria mortality and incidence across Kenya, with elevated risk concentrated in western and northwestern counties, particularly along the Lake Victoria basin and extending into parts of the Rift Valley and northeastern regions, while substantially lower levels are observed in the central highlands and southeastern counties. Incidence exhibited a broader zone of high spatial intensity than mortality, indicating more widespread transmission relative to fatal outcomes, whereas mortality appears more spatially localized, suggesting the influence of differential health-system access, treatment-seeking behavior, or comorbidity profiles across regions.

The coherence of high-burden zones between malaria incidence and mortality underscores the persistence of ecological and climatic drivers such as temperature, rainfall, and vector suitability in shaping transmission risk, while the sharper mortality gradients highlight possible disparities in health-care delivery in Kenya. These patterns align with

previous studies [6, 8, 10, 13, 17] identifying the Lake Victoria basin and coastal belt as persistent transmission zones and the highlands as low-endemic areas, confirming the established west to central gradient in Kenya's malaria epidemiology.

4.3. Fitted Models Evaluation

The diagnostic model results presented in Table 5 offer valuable insights into the performance and fit of the spatial-temporal models used for malaria incidence and mortality rates. Three key metrics are reported: the Widely Applicable Information Criterion (WAIC), the log pointwise predictive density (lppd), and the effective number of parameters (pWAIC).

Table 5. *Model Diagnostics Parameters.*

	WAIC	lppd	pWAIC
Univariate IR	4703.505	-1886.82	464.9322
Univariate MR	2822.139	-1291.267	119.8028
Multivariate Model	52468.64	-3200.416	23033.9

The univariate malaria incidence rate (IR) model had a WAIC of 4703.505, indicating moderate predictive performance, with a high pWAIC of 464.9322 suggesting complexity. The mortality rate (MR) model performs better, with a lower WAIC of 2822.139, a less negative lppd of -1291.267, and a simpler structure (pWAIC of 119.8028). The multivariate model, combining both outcomes, had a much higher WAIC of 52468.64 and a lppd of -3200.416, reflecting poorer fit due to its complexity. Overall, the univariate mortality model provides the best balance of fit and simplicity.

5. Conclusion and Recommendations

This section gives a conclusion and study recommendations for this study.

5.1. Conclusion

This study provided a comprehensive evaluation of malaria incidence and mortality in Kenya through a multivariate spatio-temporal modeling approach both for the univariate and multivariate cases. The univariate analysis revealed significant variability in malaria incidence across regions and over time while mortality rates appeared more stable. The multivariate approach offered deeper insight into the spatio-temporal dynamics of malaria incidence and mortality though its higher WAIC and pWAIC values indicated challenges in jointly modeling malaria incidence and mortality. Diagnostic assessments showed the univariate mortality model gave the best fit despite the multivariate framework remaining valuable for exploring overlapping spatial temporal variability.

5.2. Recommendations

This study notes that to make future spatial and spatio-temporal models in malaria research more accurate and reliable, it's important to include covariate data at smaller geographic areas and shorter time intervals. Furthermore, applying hierarchical Bayesian models coupled with machine learning can better handle multivariate spatial temporal relationships with non-linear effects. Additionally, future research can explore the usage of non-parametric methods or splines in multivariate spatio-temporal modeling towards giving clearer insights into how space and time relationships change over time.

ORCID

0000-0001-5740-2674 (Polycarp Okiagera Nyabuto)
0009-0009-7609-4318 (Anthony Wanjoya)
0009-0008-6195-041X (Thomas Mageto)
0009-0002-1089-6392 (Anthony Ngunyi)

Conflicts of Interest

The authors declare no conflict of interest.

References

[1] Adegbite, G., Edeki, S., Isewon, I., Emmanuel, J., Dokunmu, T., Rotimi, S., Oyelade, J., & Adebiyi, E. (2023). Mathematical modeling of malaria transmission dynamics in humans with mobility and control states. *Infectious Disease Modelling, 8*(4), 1015-1031. https://doi.org/10.1016/j.idm. 2023.08.005

[2] Agboka, K. M., Wamalwa, M., Mutunga, J. M., & Tonnang, H. E. Z. (2024). A mathematical model for mapping the insecticide resistance trend in the Anopheles gambiae mosquito population under climate variability in Africa. *Scientific Reports, 14*(1), 9850. https://doi.org/10.1038/ s41598-024-60555-z

[3] Aheto, J. M. K., Menezes, L. J., Takramah, W., & Cui, L. (2024). Modelling spatiotemporal variation in under-five malaria risk in Ghana in 2016-2021. *Malaria Journal, 23*(1), 102. https://doi.org/ 10.1186/s12936-024-04918-x

[4] Anwar, M. N., Smith, L., Devine, A., Mehra, S., Walker, C. R., Ivory, E., Conway, E., Mueller, I., McCaw, J. M., Flegg, J. A., & Hickson, R. I. (2024). Mathematical models of Plasmodium vivax transmission: A scoping review. *PLOS Computational Biology, 20*(3), e1011931. https://doi.org/10.1371/journal.pcbi.1011931

[5] Apeagyei, A. E., Patel, N. K., Cogswell, I., O'Rourke, K., Tsakalos, G., & Dieleman, J. (2024). Examining geographical inequalities for malaria outcomes and

spending on malaria in 40 malaria-endemic countries, 2010-2020. *Malaria Journal, 23*(1), 206. https://doi.org/10.1186/s12936-024-05028-4

[6] Ayele, D. G., Musa Mohammed, M. O., Abdallah, A. S. R., & Wacho, G. (2024). Assessment of Malaria Transmission in Kenya Using Multilevel Logistic Regression (SSRN Scholarly Paper 4881801). *Social Science Research Network.* https://doi.org/ 10.2139/ssrn.4881801

[7] Bationo, C. S., Gaudart, J., Dieng, S., Cissoko, M., Taconet, P., Ouedraogo, B., Somé, A., Zongo, I., Soma, D. D., Tougri, G., Dabiré, R. K., Koffi, A., Pennetier, C., & Moiroux, N. (2021). Spatio-temporal analysis and prediction of malaria cases using remote sensing meteorological data in Diébougou health district, Burkina Faso, 2016-2017. *Scientific Reports,* 11, 20027. https://doi.org/10.1038/s41598-021-99457-9

[8] Bisanzio, D., Mutuku, F., LaBeaud, A. D., Mungai, P. L., Muinde, J., Busaidy, H., Mukoko, D., King, C. H., & Kitron, U. (2015). Use of prospective hospital surveillance data to define spatiotemporal heterogeneity of malaria risk in coastal Kenya. *Malaria Journal, 14*(1), 482. https://doi.org/10.1186/s12936-015-1006-7

[9] Frings, M., Lakes, T. M., Müller, D., Khan, M. M. H., Epprecht, M., Kipruto, S., Galea, S., & Gruebner, O. (2018). Modeling and mapping the burden of disease in Kenya. *Scientific Reports,* 8, 1-9. https://doi.org/10.1038/s41598-018-28266-4

[10] Gopal, S., Ma, Y., Xin, C., Pitts, J., & Were, L. (2019). Characterizing the Spatial Determinants and Prevention of Malaria in Kenya. *International Journal of Environmental Research and Public Health,* 16. https://doi.org/10.3390/ijerph16245078

[11] Gwitira, I., Mukonoweshuro, M., Mapako, G., Shekede, M. D., Chirenda, J., & Mberikuna-she, J. (2020). Spatial and spatio-temporal analysis of malaria cases in Zimbabwe. *Infectious Diseases of Poverty, 09*(05), 45-58. https://doi.org/10.1186/s40249-020-00764-6

[12] Hamedani, G. G., Goual, H., Emam, W., Tashkandy, Y., Ahmad Bhatti, F., Ibrahim, M., & Yousof, H. M. (2023). A New Right-Skewed One-Parameter Distribution with Mathematical Characterizations, Distributional Validation, and Actuarial Risk Analysis, with Applications. *Symmetry, 15*(7), Article 7. https://doi.org/10.3390/ sym15071297

[13] Kamau, A., Mtanje, G., Mataza, C., Bejon, P., & Snow, R. W. (2021). Spatial-temporal clustering of malaria using routinely collected health facility data on the Kenyan Coast. *Malaria Journal, 20*(1), 227. https://doi.org/10.1186/s12936-021-03758-3

[14] Kang, S. Y., Battle, K. E., Gibson, H. S., Ratsimbasoa, A., Randrianarivelojosia, M., Ramboarina, S., Zimmerman, P. A., Weiss, D. J., Cameron, E., Gething, P. W., & Howes, R. E. (2018). Spatio-temporal mapping of Madagascar's Malaria Indicator Survey results to assess Plasmodium falciparum endemicity trends between 2011 and 2016. *BMC Medicine, 16*(1), 71. https://doi.org/10.1186/s12916-018-1060-4

[15] Katale, R. N., & Gemechu, D. B. (2023). Spatio-temporal analysis of malaria incidence and its risk factors in North Namibia. *Malaria Journal, 22*(1), 149. https://doi.org/10.1186/s12936-023-04577-4

[16] Katile, A., Sagara, I., Cissoko, M., Bationo, C. S., Dolo, M., Thera, I., Traore, S., Kone, M., Dembele, P., Bocoum, D., Sidibe, I., Simaga, I., Sissoko, M. S., Landier, J., & Gaudart, J. (2022). Spatio-Temporal Variability of Malaria Incidence in the Health District of Kati, Mali, 2015-2019. *International Journal of Environmental Research and Public Health, 19*(21), Article 21. https:// doi.org/10.3390/ijerph192114361

[17] Khagayi, S., Amek, N., Bigogo, G., Odhiambo, F., & Vounatsou, P. (2017). Bayesian spatio-temporal modeling of mortality in relation to malaria incidence in Western Kenya. *PLOS ONE, 12*(7), e0180516. https://doi.org/10.1371/journal.pone.0180516

[18] Khan, A., Bisanzio, D., Mutuku, F., Ndenga, B., Grossi-Soyster, E. N., Jembe, Z., Maina, P. W., Chebii, P. K., Ronga, C. O., Okuta, V., & LaBeaud, A. D. (2023). Spatiotemporal overlapping of dengue, chikungunya, and malaria infections in children in Kenya. *BMC Infectious Diseases, 23*(1), 183. https://doi.org/10.1186/s12879-023-08157-4

[19] Kimuyu, J. S. (2021). Comparative spatial-temporal analysis and predictive modeling of climate change-induced malaria vectors' invasion in new hotspots in Kenya. *SN Applied Sciences, 3*(8), 741. https://doi.org/10.1007/s42452-021-04722-1

[20] Kitawa, Y. S., Johnson, O., Giorgi, E., & Asfaw, Z. G. (2023). Understanding the importance of spatial correlation in identifying spatio-temporal variation of disease risk, in the case of malaria risk mapping in southern Ethiopia. *Scientific African,* 22, e01926. https://doi.org/10.1016/ j.sciaf.2023.e01926

[21] Liu, M., Liu, Y., Po, L., Xia, S., Huy, R., Zhou, X.-N., & Liu, J. (2023). Assessing the spatiotemporal malaria transmission intensity with heterogeneous risk factors: A modeling study in Cambodia. *Infectious Disease Modelling, 8*(1), 253. https://doi.org/ 10.1016/j.idm.2023.01.006

[22] Maiti, M., & Roy, U. (2024). Space-time clusters and co-occurrence of Plasmodium vivax and Plasmodium falciparum malaria in West Bengal, India. *Malaria*

Journal, 23(1), 189.
https://doi. org/10.1186/s12936-024-05015-9

[23] Mandal, B., & Mondal, S. (2024). Unveiling spatio-temporal mysteries: A quest to decode India's Dengue and Malaria trend (2003-2022). *Spatial and Spatio-Temporal Epidemiology, 25* (1), 100690.
https://doi.org/10.1016/j.sste.2024.100690

[24] Mougeni, F., Lell, B., Kandala, N.-B., & Chirwa, T. (2024). Bayesian spatio-temporal analysis of malaria prevalence in children between 2 and 10 years of age in Gabon. *Malaria Journal, 23*(1), 57.
https://doi.org/10.1186/s12936-024-04880-8

[25] Muzame, B. A., Omukunda, E., Mulama, D., & Okoth, P. (2024). Spatio-temporal characterization of malaria prevalence in a peri-urban resource limited setting of Western Kenya Highlands. *African Health Sciences, 24*(3), Article 3. https://doi.org/ 10.4314/ahs.v24i3.14

[26] Nyawanda, B. O., Khagayi, S., Obor, D., Odhiambo, S. B., Beloconi, A., Otieno, N. A., Bigogo, G., Kariuki, S., Munga, S., & Vounatsou, P. (2024). The effects of climatic and non-climatic factors on malaria mortality at different spatial scales in western Kenya, 2008-2019. *BMJ Global Health, 9*(9), e014614.
https://doi.org/10.1136/bmjgh-2023-014614

[27] Odhiambo, J. N., Kalinda, C., Macharia, P. M., Snow, R. W., & Sartorius, B. (2020). Spatial and spatio-temporal methods for mapping malaria risk: A systematic review. *BMJ Global Health, 5*(10), e002919.
https://doi.org/10.1136/bmjgh-2020-002919

[28] Ogunsakin, R. E., Babalola, B. T., Olusola, J. A., Joshua, A. O., & Okpeku, M. (2024). GIS-based spatiotemporal mapping of malaria prevalence and exploration of environmental inequalities. *Parasitology Research, 123*(7), 262.
https://doi.org/10. 1007/s00436-024-08276-0

[29] Quick, H., Song, G., & Tabb, L. P. (2021). Evaluating the informativeness of the Besag-York-Mollié CAR model. *Spatial and Spatio-Temporal Epidemiology,* 37, 100420.
https://doi.org/10.1016/ j.sste.2021.100420

[30] Rotejanaprasert, C., Lawpoolsri, S., Sa-angchai, P., Khamsiriwatchara, A., Padungtod, C., Tipmontree, R., Menezes, L., Sattabongkot, J., Cui, L., & Kaewkungwal, J. (2023). Projecting malaria elimination in Thailand using Bayesian hierarchical spatiotemporal models. *Scientific Reports, 13*(1), 7799.
https://doi.org/10.1038/s41598-023-35007-9

[31] Sangaré, I., Ouattara, C. A., Soma, D. D., Soma, D., Assogba, B. S., Namountougou, M., Tougri, G., & Savadogo, L. B. (2022). Spatial-temporal pattern of malaria in Burkina Faso from 2013 to 2020. *Parasite Epidemiology and Control,* 18, e00261.
https://doi.org/10.1016/j.parepi.2022.e00261

[32] Selemani, M., Mrema, S., Shamte, A., Shabani, J., Mahande, M. J., Yeates, K., Msengwa, A. S., Mbago, M. C. Y., & Lutambi, A. M. (2015). Spatial and space-time clustering of mortality due to malaria in rural Tanzania: Evidence from Ifakara and Rufiji Health and Demographic Surveillance System sites. *Malaria Journal, 14*(1), 369.
https://doi.org/10.1186/s12936-015-0905-y

[33] Wang, C., Thakuri, B., Roy, A. K., Mondal, N., Qi, Y., & Chakraborty, A. (2023). Changes in the associations between malaria incidence and climatic factors across malaria endemic countries in Africa and Asia-Pacific region. *Journal of Environmental Management,* 331, 117264. https://doi. org/10.1016/j.jenvman.2023.117264

[34] Wang, G. (2022). Laplace approximation for conditional autoregressive models for spatial data of diseases. *MeodsXth,* 9, 101872.
https://doi.org/10.1016/j.mex.2022.101872